Georgia Institute of Technology

CRMP

CRMP-2015-12-001

Whitepaper

The Current Status of the Tools for Modeling and Simulation of Advanced High Temperature Reactor Neutronics Analysis

Computational Reactor and Medical Physics Laboratory
Nuclear and Radiological Engineering Programs
Georgia Institute of Technology
Atlanta, GA 30332

Issue Date: December 11, 2015

FOR PUBLIC DISTRIBUTION

Whitepaper

The Current Status of the Tools for Modeling and Simulation of Advanced High Temperature Reactor Neutronics Analysis

Prepared by:

Farzad Rahnema
Bojan Petrovic
Christopher Edgar
Dingkang Zhang
Pietro Avigni
Michael Huang
Stefano Terlizzi
Georgia Institute of Technology, Atlanta, Georgia

Acknowledgement

This work is being performed using funding received from the U.S. Department of Energy Office of Nuclear Energy's Nuclear Energy University Programs.

Executive Summary

A team of researchers, led by the Georgia Institute of Technology (GT), and including major collaborators from The Ohio State University (OSU), Texas A&M University (TAMU), Texas A&M University Kingsville (TAMU-K), Oak Ridge National Laboratory (ORNL), and AREVA, as well as international partners at University of Zagreb, Politecnico di Milano, and Shanghai Institute of Applied Physics (SINAP) were selected by the U.S. Department of Energy to form an Integrated Research Project (IRP) exploring Fluoride High-Temperature Reactor (FHR) technology and licensing challenges. The GT led IRP chose the ORNL preconceptual design for the Advance High Temperature Reactor (AHTR) as its candidate design for analysis and technology development. An additional IRP, led by the Massachusetts Institute of Technology (MIT) was also funded and focuses on a different FHR reactor design.

One area of major concern is the verification and validation (V&V) of neutronics tools, codes, and methodologies for core and system design in support of licensure of FHRs. In order to begin addressing this task, the GT led IRP has decided to hold a Phenomena Identification and Ranking Table (PIRT) panel with internal and invited external experts to address issues related to the V&V of neutronics tools, codes, and methodologies. The first PIRT panel scheduled for the FHR-IRP on neutronics will take place on December 8-10, 2015 at Georgia Tech. The panel will be led by David Diamond, and consists of both internal and external experts on neutronics, modeling and simulation, salt and graphite properties, and other areas of interest for FHR technologies. Student observers with an interest in neutronics or neutronics related activities are expected to attend the PIRT exercise from both the GT and MIT led IRPs.

This whitepaper was commissioned to provide a starting point of reference for the internal and invited external experts as they prepare for the PIRT exercise. The most recent revision of the AHTR preconceptual design is presented, with an emphasis on reactor components relevant to neutronics simulations. Parameters and quantities of interest based on previous neutronics analysis of the AHTR and systems sharing similar physics are presented. Finally, an initial list of gaps and areas of concern have been complied to provide a starting point for discussions by the PIRT. This initial list does not represent all phenomena the panel will address, and may include some items which are deemed to have minimal impact on relevant neutronics phenomena.

Table of Contents

List of Figures

List of Tables

List of Abbreviations

AGR	Advanced Gas Reactor
AHTR	Advanced High Temperature Reactor
C-C	Carbon-Carbon
CHM	Carbon to Heavy Metal
DOE	U.S. Department of Energy
DRACS	Direct Reactor Auxiliary Cooling System
FHR	Fluoride High Temperature Reactor
GT	Georgia Institute of Technology
HTGR	High Temperature Gas Reactor
IRP	Integrated Research Project
NEUP	Nuclear Energy University Programs
OD	Outer Diameter
ORNL	Oak Ridge National Laboratory
OSU	The Ohio State University
PBR	Pebble Bed Reactor
PIRT	Phenomena Identification and Ranking Table
RPT	Reactivity-Equivalent Physical Transformation
RSICC	Radiation Safety Information Computational Center
SINAP	Shanghai Institute of Applied Physics
TAMU	Texas A&M University
TAMU-K	Texas A&M University, Kingston
TRISO	Tristructural-Isotropic
VHTR	Very High Temperature Reactor
V&V	Verification and Validation

1. Introduction

The widespread deployment of Fluoride High-Temperature Reactor (FHR) technology promises many benefits: improved safety through passive safety systems and proliferation-resistant waste forms; improved economics through higher operating temperatures and thus higher operating efficiency; and a diversification of the nation's energy portfolio by expanding the role of nuclear power beyond baseload electricity to meeting peaking electricity demand and supplying industrial process heat. Several challenges remain before this class of reactors can be deployed, mostly related to its technological readiness. Realizing this need, the U.S. Department of Energy (DOE) initiated and Integrated Research Project (IRP) to address the technology gaps for FHR deployment.

A team of researchers, led by the Georgia Institute of Technology (GT), and including major collaborators from The Ohio State University (OSU), Texas A&M University (TAMU), Texas A&M University Kingsville (TAMU-K), Oak Ridge National Laboratory (ORNL), and AREVA, as well as international partners at University of Zagreb, Politecnico di Milano, and Shanghai Institute of Applied Physics (SINAP) were selected to form one of the IRPs exploring FHR technology and licensing challenges. The GT led IRP chose the ORNL preconceptual design for the Advance High Temperature Reactor (AHTR) as its candidate design for analysis and technology development. An additional IRP, led by the Massachusetts Institute of Technology (MIT) was also funded and focuses on a different FHR reactor design.

One area of major concern is the verification and validation (V&V) of neutronics tools, codes, and methodologies for core and system design in support of licensure of FHRs. In order to begin addressing this task, the GT led IRP has decided to hold a Phenomena Identification and Ranking Table (PIRT) panel with internal and invited external experts to address issues related to the V&V of neutronics tools, codes, and methodologies. The first PIRT panel scheduled for the FHR-IRP on neutronics will take place on December 8-10, 2015 at Georgia Tech. The panel will be led by David Diamond, and consists of both internal and external experts on neutronics, modeling and simulation, salt and graphite properties, and other areas of interest for FHR technologies. Student observers with an interest in neutronics or neutronics related activities are expected to attend the PIRT-like exercise from both the GT and MIT led IRPs.

As a starting point for the panelists, a whitepaper on *The Current Status of the Tools for Modeling and Simulation Tools for Advanced High Temperature Reactor Neutronics Analysis* has been compiled to perform the following roles in preparation for the meeting:

- Present the AHTR Design Concept
- Identify parameters and quantities of interest for neutronics (e.g. k_{eff}, cross-section uncertainty, reactivity coefficients, etc.)
- Discuss any previous neutronics related work for the AHTR
- Identify any gaps in parameters or quantities and areas of concern for neutronics modeling and simulation

2. Review of the AHTR Conceptual Design

As a preliminary step leading up to the PIRT panel on neutronics, researchers at Georgia Tech have developed a definition of a reference AHTR primary system and core design, to be utilized for benchmarking purposes. The design presented in the subsequent sections is not optimized, but provides an excellent reference/starting point for code cross-validation and further evaluations and optimization. A definition of all geometric and material properties has been developed, based on work from ORNL and other related projects over the last 10+ years. The general design of the AHTR is presented in two ORNL reports; both reports use slightly different numbers for specific design parameters, because the most recent design has been partially optimized. (Holcomb, et al., 2011) (Varma, et al., 2012) The most recent design was considered to be the reference design for general parameters, however some features which were not full defined in the most recent report were obtained from the initial, non-optimized design.

2.1. General Overview of the Plant Design

The Advanced High-Temperature Reactor (AHTR) was designed to have a power of 3400 MW_{th} and an efficiency of approximately 45%, corresponding to a power of 1530 MW_e. The AHTR design concept is a Fluoride High-Temperature Reactor (FHR) with a primary coolant of FLiBe ($2LiF\text{-}BeF_2$), coupled to an intermediary salt loop containing $Kf\text{-}Zr\text{-}F_4$. The power cycle is based on the supercritical water cycle, with the water loop coupled to the intermediary salt loop. The AHTR exploits passive safety systems, such as Direct Reactor Auxiliary Cooling System (DRACS), in order to minimize the requirements for external support during accident scenarios. A general plant overview is presented in Figure 2-1.

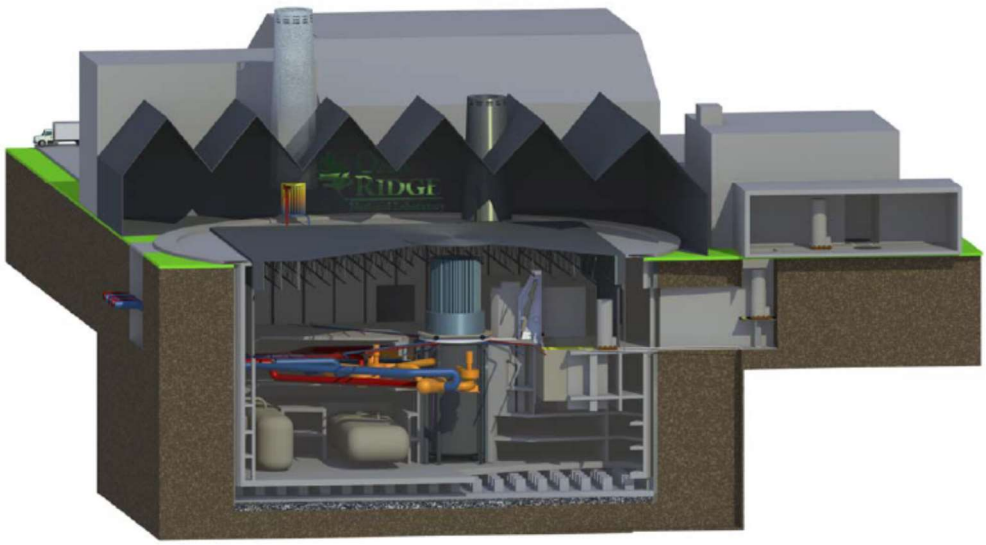

Figure 2-1: Overview of the AHTR plant design. (Varma, et al., 2012)

The reactor fuel is based on the Tristructural-Isotropic (TRISO) particles and is in the form of a layered uranium oxy-carbide (UCO) material. The most recent design from ORNL calls for a fuel enrichment of 9 wt%, though an enrichment of 19.75 wt% was called for in the original preconceptual design. (Holcomb, et al., 2011) (Varma, et al., 2012) The core consists of these TRISO particles loaded into 252 active fuel assemblies containing 18 fuel plates each, arranges such that the assembly is hexagonal. The active height of the AHTR core is 5.5 m and utilizes graphite for both moderation and reflection of neutrons.

The primary reactor coolant salt is FLiBe, which undergoes a temperature increase of 50°C on average, across the core (including the bypass flow). The core inlet temperature is 650°C and the outlet is 700°C. From the design parameters, one can calculate the mass flow rate of FLiBe (assuming the average specific heat of the coolant is 2,415 J/kg·K) to be approximately 28,150 kg/s. The reactor vessel is not pressurized.

Table 2-1: General AHTR plant parameters.

Parameter	Value	Units
Core Thermal Power	3,400	MW
Overall Thermal Efficiency	45%	-
Fuel Type	TRISO	-
Uranium Composition	UCO	-
Number of Fuel Assemblies	252	-
Moderator and Reflector Material	Graphite	-
Active Core Height	5.5	m
Primary Coolant Salt	FLiBe	-
Core Inlet Temperature	650	°C
Core Outlet Temperature	700	°C

Further details on the core specifications will be provided in the subsequent sections of this document. Additionally, general information about the intermediate salt loop, power cycle, and decay heat removal system can be found in the ORNL preconceptual/conceptual design documents. (Holcomb, et al., 2011) (Varma, et al., 2012)

2.2. Reactor Vessel and Out-of-Core Structure

This section describes the AHTR reactor vessel and some components of the out-of-core structure. The reactor vessel is roughly cylindrical in nature and hung from its upper flange, to minimize the stress incurred by the thermal expansion. (Varma, et al., 2012) Figure 2-2 depicts the basic overview of the AHTR vessel and core location.

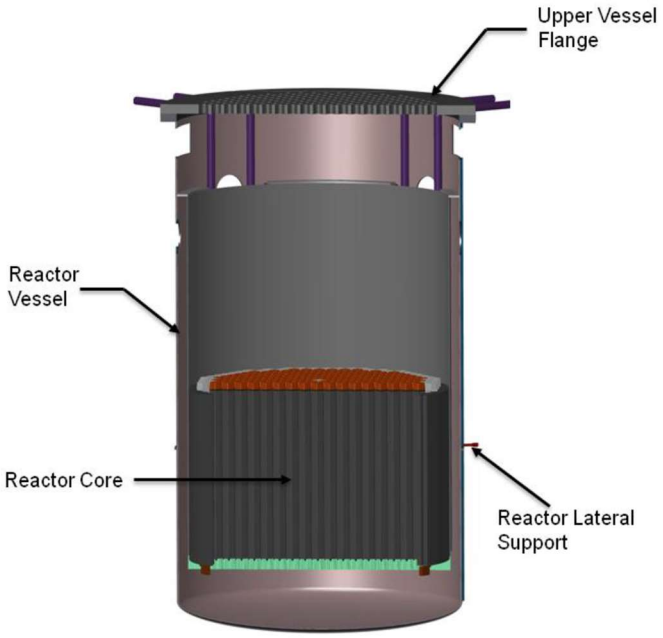

Figure 2-2: AHTR reactor vessel cross section. (Varma, et al., 2012)

Table 2-2 provides the global parameters of the AHTR reactor vessel, which is made from 800-H alloy and has a yield strength of 20 MPa at 700°C. There is a possibility of corrosion with the FLiBe coolant and the 800-H alloy, thus a thin (1 cm thick) liner of Alloy-N is included on surfaces contacting the FLiBe. The vessel thickness is not defined in the ORNL reference reports. However, it is assumed to be 5 cm, though from a mechanical standpoint a larger thickness may be required.

Table 2-2: Global parameters of the AHTR reactor vessel.

Parameter	Value	Units
Exterior Vessel Diameter	10.5	m
Vessel Height	19.1	m
Primary Salt Depth Above Upper Support Plate	7.15	m
Primary Piping Interior Diameter	1.24	m
Number of DRACS	3	-
Core Barrel Material	C-C Composite	-
Vessel and Primary Piping Material	800-H Alloy w/Alloy-N Lining	-

The full reactor vessel configuration can be observed in Figure 2-3, and depicts the location of the refueling lobe. The vessel size exceeds the limits for transportation by rail, thus the vessel must be transported to the site in sections and welded into the final vessel. (Varma, et al., 2012)

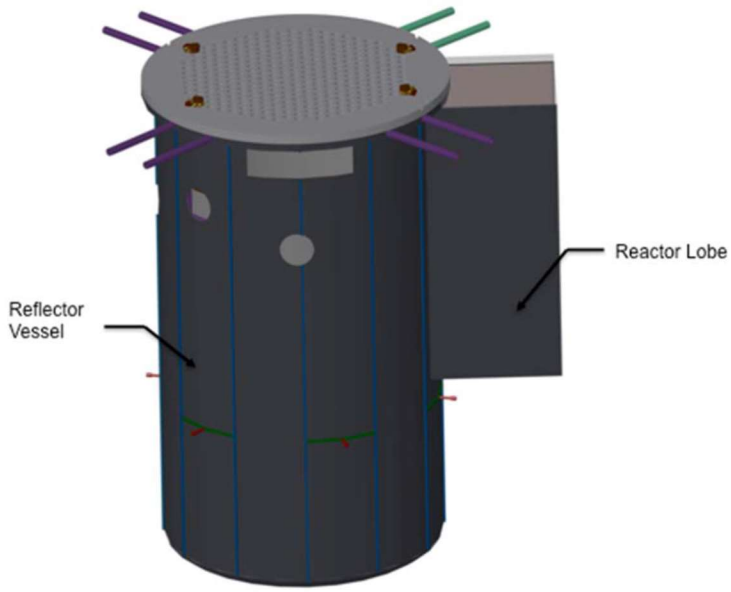

Figure 2-3: AHTR reactor vessel. (Varma, et al., 2012)

2.2.1. Upper Plenum

The upper plenum is delimited by the upper support plate and the reactor vessel flange. The upper portion of the plenum is filled with Argon cover gas (not pressurized) at a temperature of 250°C. The cover gas volume has a height of 3.19 m. The lower portion of the upper plenum (Figure 2-4) is filled with FLiBe coming from the core, at an average temperature of 700°C. The salt is 7.15 m deep from the upper core plate. During normal operation, guide tubes for leader rods occupy the upper plenum. These rods are retractable, in order to provide access for refueling.

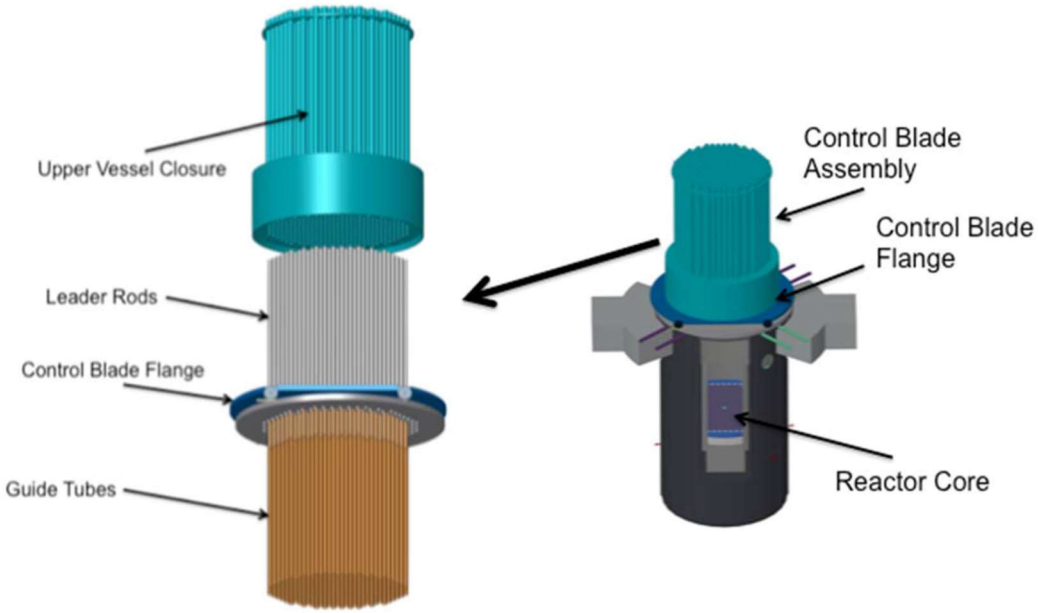

Figure 2-4: AHTR upper plenum, guide tubes, and the upper vessel closure. (Varma, et al., 2012)

2.2.2. Top Flange

The top flange (Figure 2-5) has a diameter of 11.6 m and a thickness of 35 cm, consisting of a truss structure fabricated by two 1.5 cm thick stainless steel top and bottom plates (to reduce weight). The volume fraction of the solid material is 13.45% of a reference cylinder that wraps the flange. The flange is maintained at a temperature of 250°C by the Argon gas in the upper portion of the upper plenum.

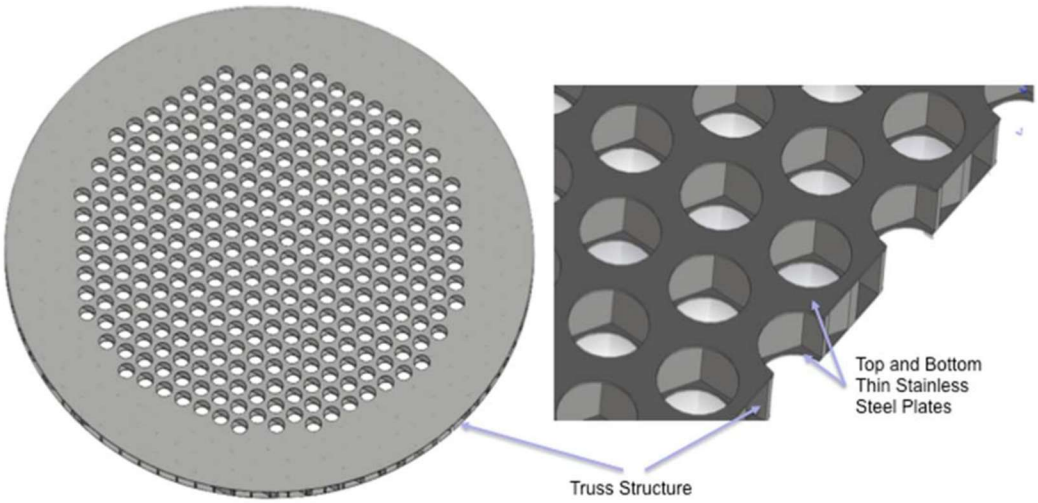

Figure 2-5: AHTR top flange configuration. (Varma, et al., 2012)

2.3. Core Barrel and Downcomer

The core barrel separates the core from the downcomer/DRACS heat exchanger region and is made up of a 2 cm thick Carbon-Carbon (C-C) composite. The interior face (towards the core) of the barrel has a thin plating of boron carbide (thickness 1 cm), which attenuates neutron radiation before it impacts the reactor vessel. The internal diameter of the core barrel is 9.56 m and the outer diameter is 9.62 m, resulting in a core barrel that is 6 cm thick. The operating temperature is 650°C (same as inlet core temperature) and flow direction is downward in the downcomer region (upward in the core). The downcomer region is subdivided azimuthally into 8 angular zones; 3 downcomer sections, 3 DRACS sections, 1 maintenance cooling system, and a 1 refueling lobe. Figure 2-6 depicts the core barrel and downcomer regions of the AHTR.

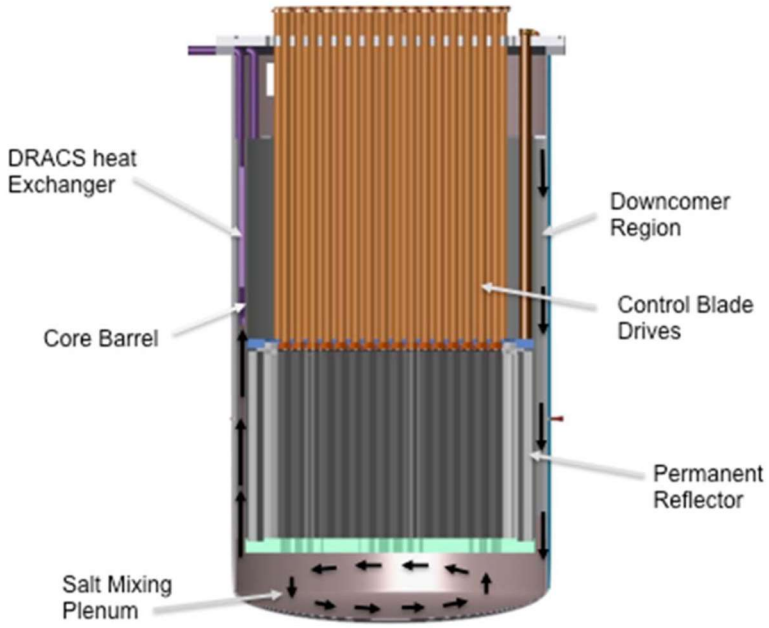

Figure 2-6: Vertical cross section of the AHTR reactor vessel and core, showing the downcomer region and core barrel. (Varma, et al., 2012)

2.4. Reactor Core

The reactor core contains 252 fuel assemblies arranged hexagonally. The central assembly is not fueled, but serves as a moderator block (it has the same composition and structure as the outer removable reflector blocks). The gap between assemblies is 1.8 cm and the equivalent diameter of the reactor core is 7.81 m for the fueled part. One ring of replaceable reflector assemblies surrounds the last ring of fueled assemblies, and then a permanent reflector completes the core. The equivalent diameter of the core including the replaceable reflector is 8.69 m. The outer radius of the permanent reflector is 9.56 m.

The core height is 6 m, of which 5.5 m is the active core; top and bottom nozzle/reflector regions are 25 cm each, the support plates are 35 cm thick, resulting in an overall height of 6.7 m for the core and support plates. Figure 2-7 provides a view of the core reflectors, upper support plate and lower support plate. Figure 2-8 depicts a horizontal cross section of the core through the fuel midplane.

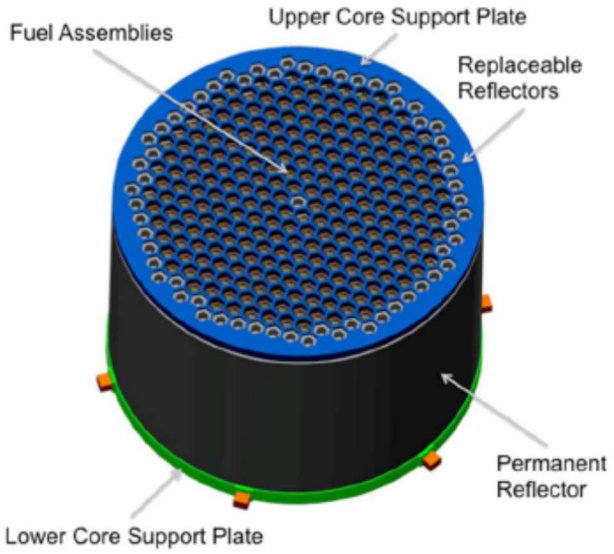

Figure 2-7: AHTR core reflector, upper support plate, and lower support plate. (Varma, et al., 2012)

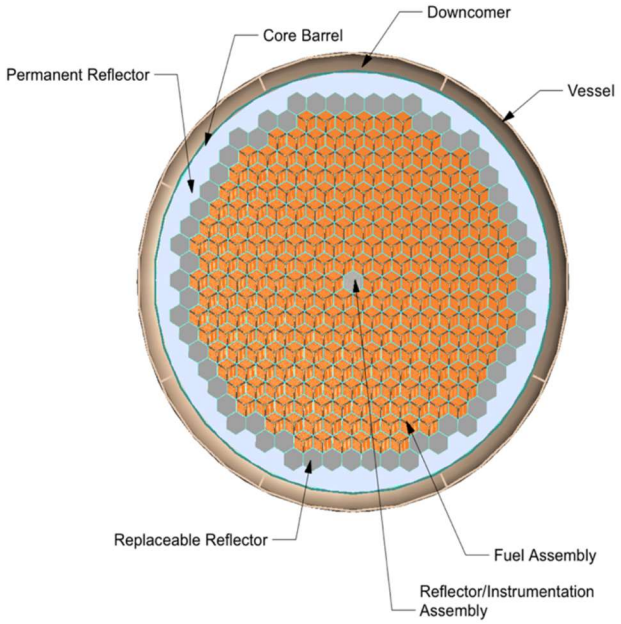

Figure 2-8: AHTR core horizontal cross section through fuel midplane. (Varma, et al., 2012)

2.4.1. Replaceable Reflector

The replaceable reflector surrounds the outermost fuel assembly ring and consists of a single ring of removable reflector blocks (shown as dark gray in Figure 2-8). The replaceable reflector blocks are made of graphite and have the same size and shape as the fueled assemblies. In the reference design they are not provided with control rods. However, in principle a control rod could be added to each reflector block to facilitate the control of the reactor power. No coolant channels are present in the reflector block, but they could be added if cooling is required.

2.4.2. Permanent Reflector

The permanent reflector surrounds the removable reflector ring and consists of solid graphite sections (depicted as light grey in Figure 2-8). Its shape conforms to the replaceable reflector blocks on the inner side and has a cylindrical outer shape that conforms to the core barrel.

2.4.3. Lower Support Plate

The lower support plate provides support to the core and reflector. It is a honeycomb structure that is attached to the reactor vessel through lateral junctions. The lower support plate is made of SiC-SiC composite and is 35 cm thick. Channel cuts have been made in the lower plate to direct the flow of FLiBe into the fuel assemblies (Figure 2-9). Additionally, indexing holes and guides provide for proper alignment of fuel assemblies during refueling operations.

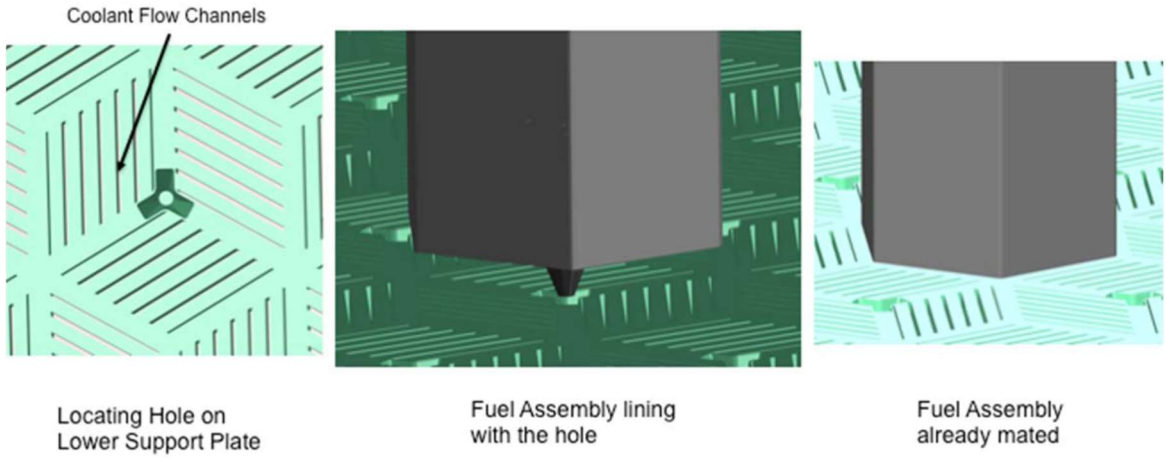

Figure 2-9: Detailed representation of the AHTR lower support plate. (Varma, et al., 2012)

For neutronics modeling purposes, as simplified model of the lower support plate can be represented by a cylinder of the same dimensions made of 14.96% FLiBe and 85.04% graphite, by volume at a temperature of 650°C.

2.4.4. Upper Support Plate

The upper support plate's primary function is to hold core components in place, against the upward flowing salt. The upper support plate is 35 cm thick and made of a SiC-SiC composite (same material as the lower support plate). Four drive rods are used to raise and lower the upper support plate during refueling outages. Figure 2-10 depicts the location of the upper support plate and the location of the drive rods in the salt filed portion of the upper plenum.

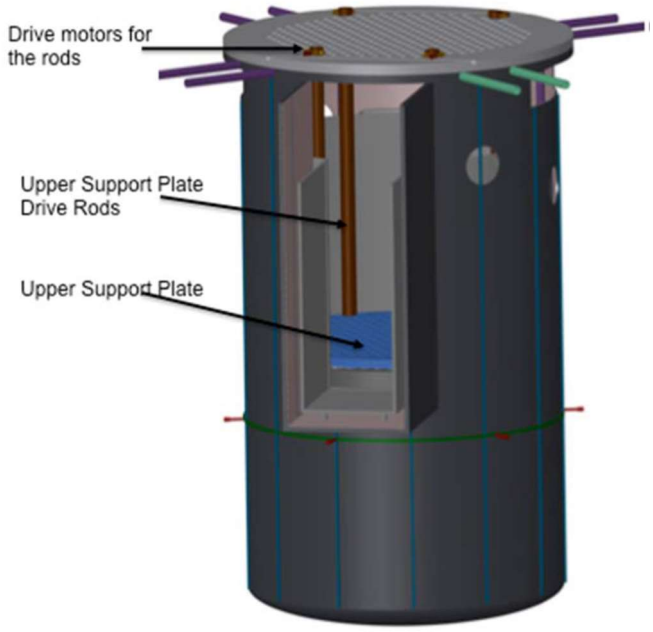

Figure 2-10: View of the salt filled portion of the upper plenum and the drive rods for the upper support plate. (Varma, et al., 2012)

The upper support plate makes tangential contact with the hemispherical contacts on the grappling collar of the fuel assemblies (Figure 2-11). The webbing on the upper core support plate fills the inter-assembly gap and provides a reduction in flow vibrations. For neutronics modeling purposes, as simplified model of the upper support plate can be represented by a cylinder of the same dimensions made of 78.9% FLiBe and 21.1% graphite, by volume at a temperature of 700°C.

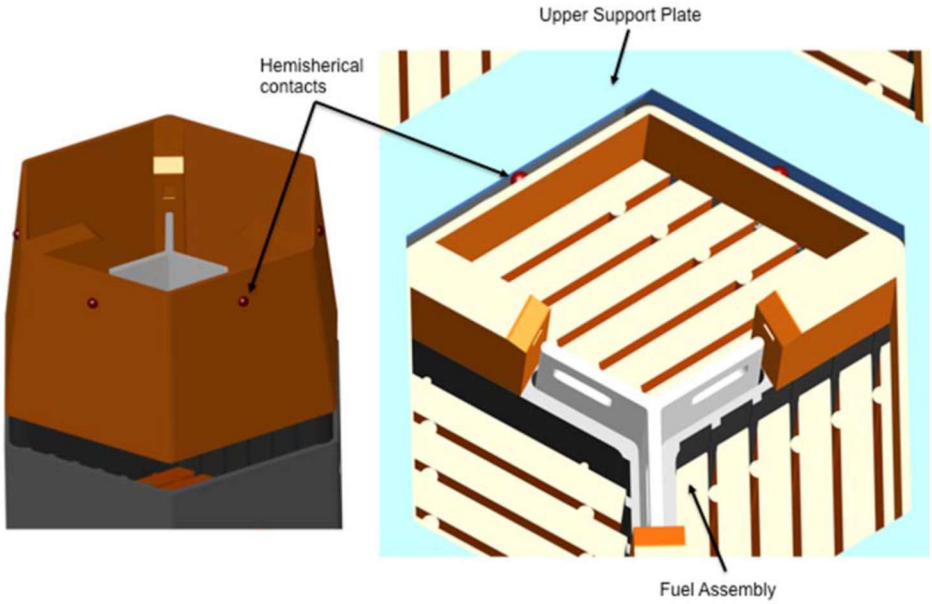

Figure 2-11: Contact between the AHTR fuel assembly grappling collar and the upper support plate. (Varma, et al., 2012)

2.4.5. Consolidated AHTR Core and Vessel Dimensions

This section provides a consolidated placement of the overall dimensions of the major components in the AHTR vessel and core. Some parameters have been assumed, since they are not fully specified in the ORNL preconceptual AHTR design description. Table 2-3 provides the outer diameters (OD) of the various vessel components. The following assumptions were made in preparation of these dimensions:

- The height of the lower plenum is assumed to be 2 m; this results in a cover gas volume height of 3.19 m. Increasing the lower plenum height results in a decreased cover gas volume height in the upper plenum.
- The reactor vessel thickness is 5 cm, plus a 1 cm Alloy-N liner.
- The height of the downcomer (with respect to the lower face of the lower support plate, corresponding to the top of the lower plenum) is assumed to be 13 m.

Table 2-3: AHTR vessel and core component outer diameters (OD). (Varma, et al., 2012)

Parameter	Value	Units
Core OD	7.81	m
Replaceable Reflector Equivalent OD	8.69	m
Permanent Reflector Equivalent OD	9.56	m
Boron Layer OD	9.58	m
Barrel OD	9.62	m
Downcomer OD	10.38	m
Alloy-N Liner OD	10.40	m
Vessel OD	10.50	m

Figure 2-12 presents the major vessel and core dimensions, while Figure 2-13 and Figure 2-14 provide an enhanced view of the top of the downcomer and top of the core, respectively.

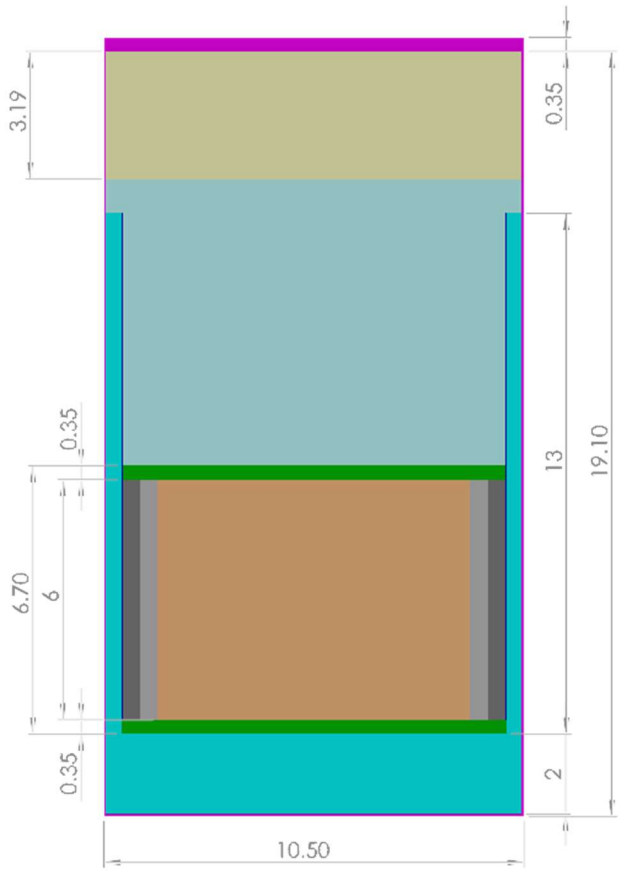

Figure 2-12: AHTR vessel and core major dimensions in meters.

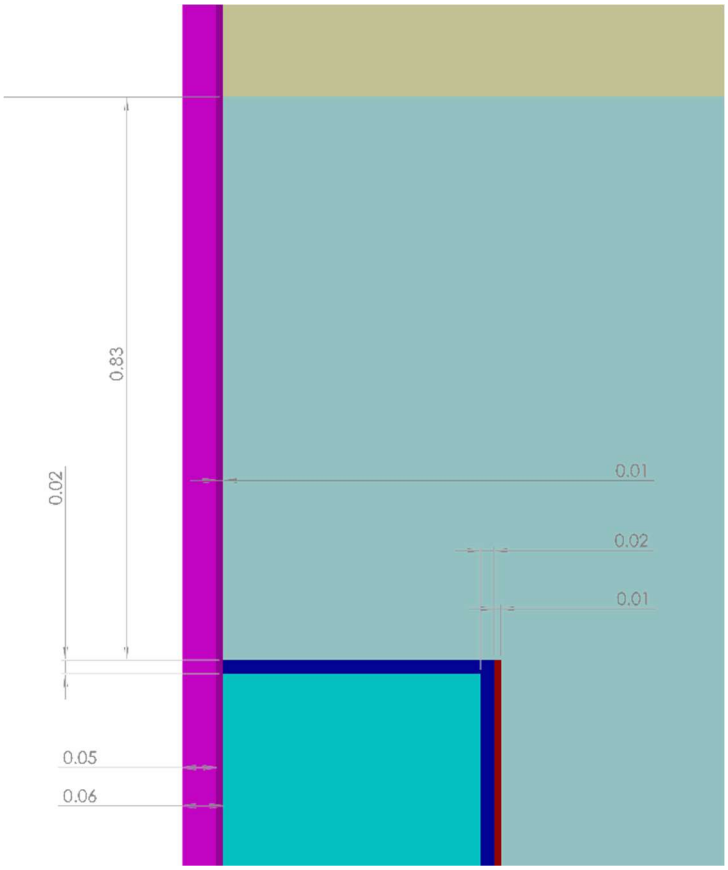

Figure 2-13: Enhanced view of dimensions at the top of the AHTR downcomer.

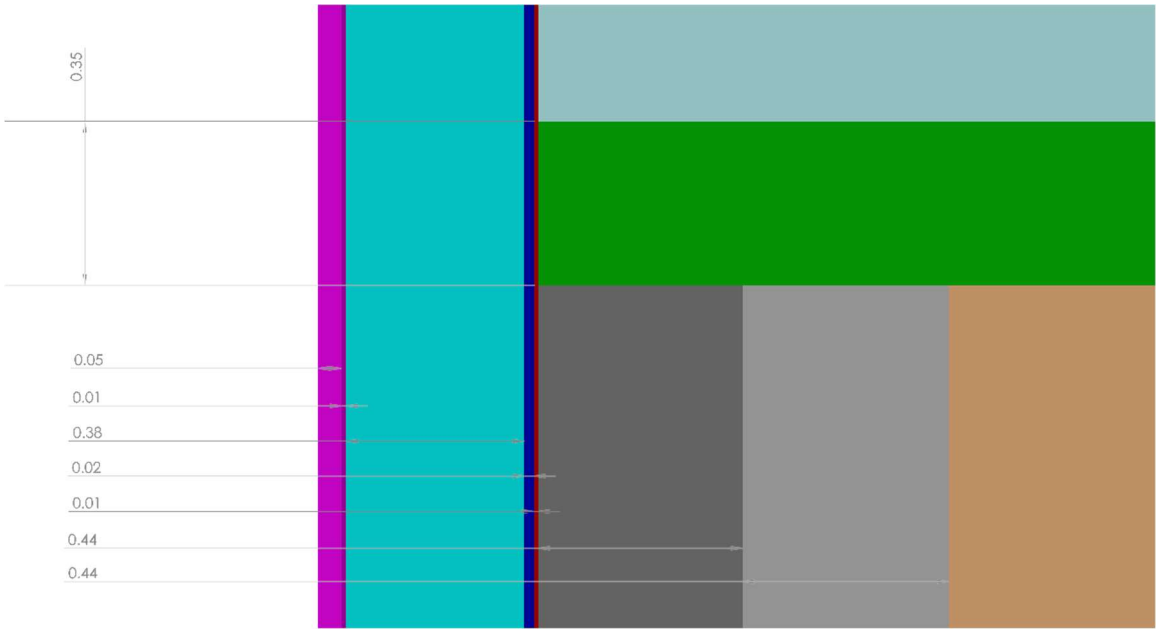

Figure 2-14: Enhanced view of dimensions at the top of the AHTR core.

2.5. Fuel Assembly

Fuel assemblies are made up of 18 fuel plates, grouped in 3 clusters of 6 plates each. Each plate is 2.55 cm thick. The entire fuel assembly is fabricated with high temperature materials. The plates in the assembly are 6 m long, the active (fueled) part is 5.5 m (of the total 6 m), and the remaining part (25 cm on top and bottom) are made of reflector material. These plates are enclosed in a hexagonal C-C fuel channel box (density 1.95 g/cm^3), which is 1 cm thick. The outer apothem of the box is 22.5 cm, corresponding to 45 cm distance between two parallel outer faces of the box wall. The three symmetric regions (groups of plates) are separated by a Y shaped support structure that is 4 cm thick and made of C-C composite (density 1.95 g/cm^3). The coolant channels are 0.7 cm thick, except for the first and last channel of every region, which are half of the full thickness (0.35 cm). Figure 2-15 shows the reference dimensions of the horizontal cross section of the assembly, while Figure 2-16 shows some dimensions that can be derived from the reference dimensions. A three dimensional view of the fuel assembly structure is given in Figure 2-17.

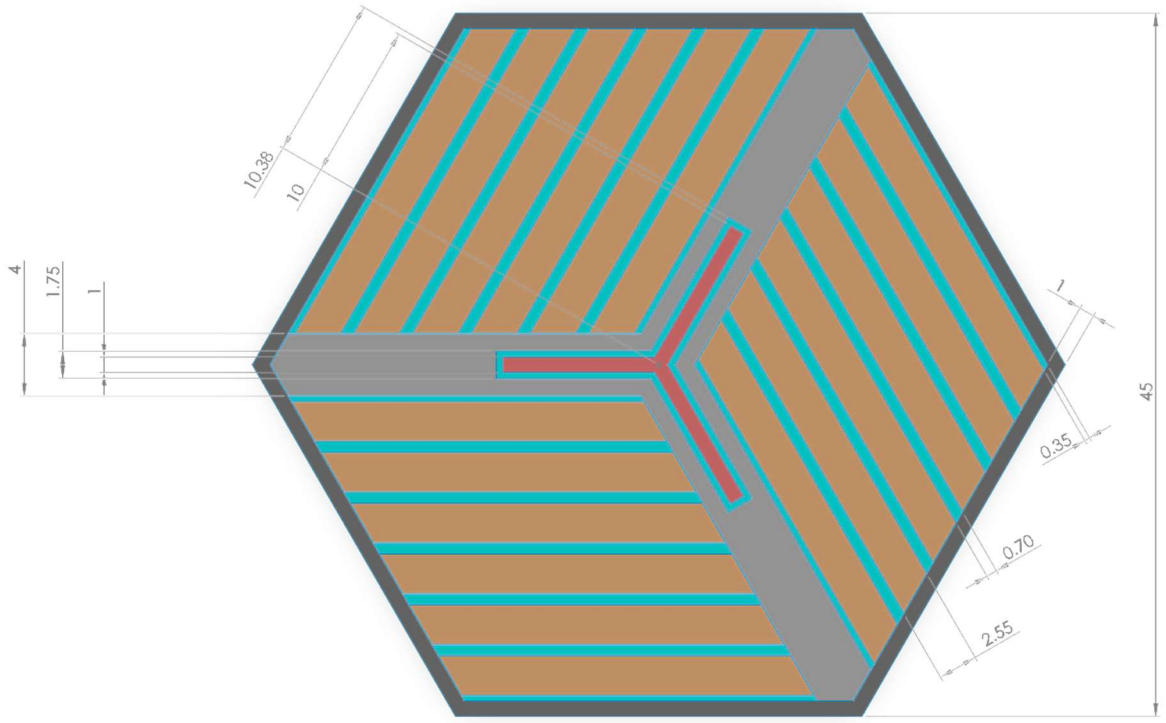

Figure 2-15: AHTR fuel assembly reference dimensions. (Varma, et al., 2012)

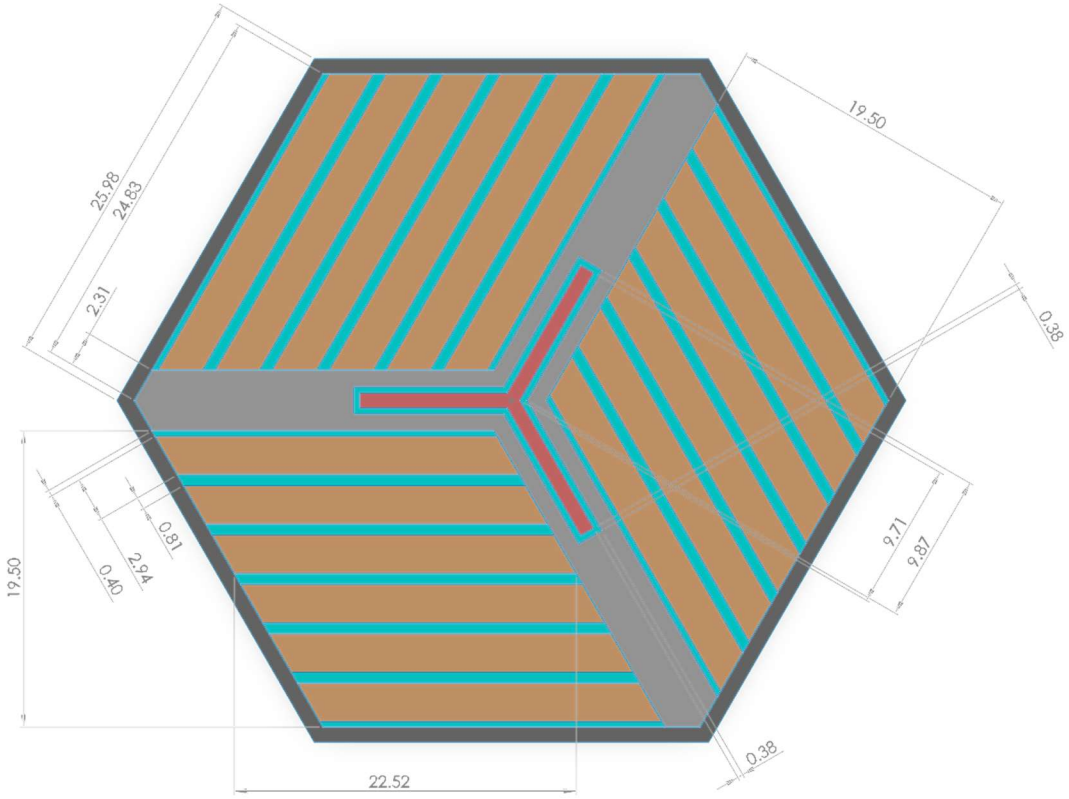

Figure 2-16: AHTR fuel assembly derived dimensions. (Varma, et al., 2012)

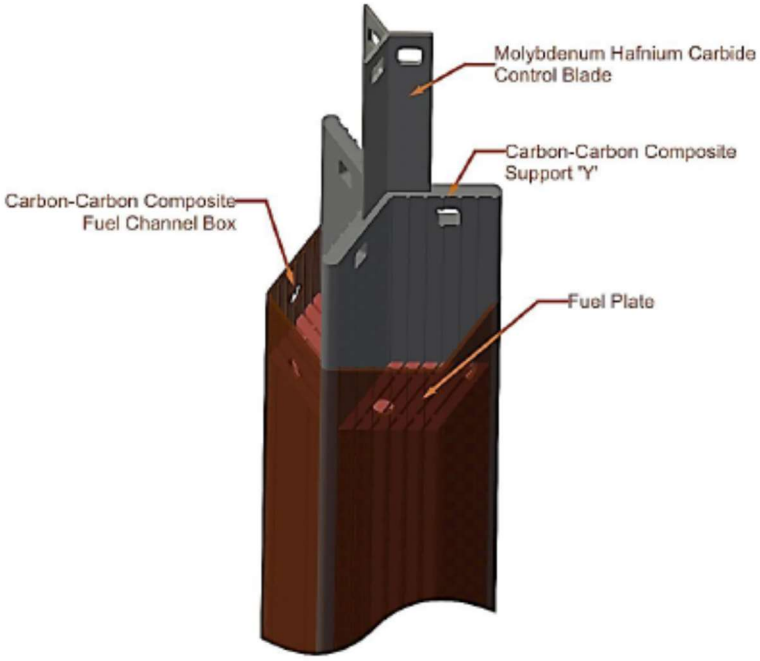

Figure 2-17: AHTR fuel assembly, 3-D view. (Varma, et al., 2012)

The gap between nearby assemblies is 1.8 cm, in order to accommodate for any mechanical distortion. The triangular fuel assembly pitch is then 46.8 cm. Figure 2-18 shows the horizontal cross section of 7 nearby assemblies.

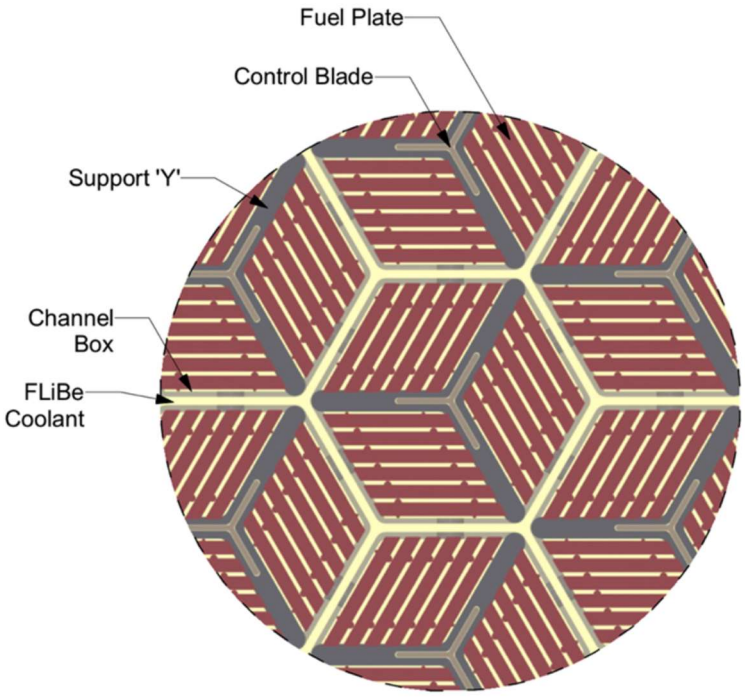

Figure 2-18: Horizontal positioning of the assemblies in the core. (Varma, et al., 2012)

2.5.1. Control Blade

Each fuel assembly has its own control blade, with relatively low worth per rod. The Y-shaped control rod is made of molybdenum hafnium carbide (MHC) and is inserted into a central Y-shaped support. The MHC is a commercial, particle-strengthened molybdenum-based allow with 1.2 wt% Hafnium and 0.1 wt% Carbon, with a density of 10.28 g/cm^3. The leader rod attaches at the top of the control rod, using the grappling holes, and serves to move the control rod up and down. The Y-shaped control blade slot dimensions are 10.38 cm long for each wing (with respect to the center of the assembly) and 1.75 cm thick. This allows for the Y-shaped control blade to be inserted, which has dimensions of 10 cm long for each wing (with respect to the center of the assembly) and 1 cm thick. Figure 2-19 shows the AHTR control blade geometry.

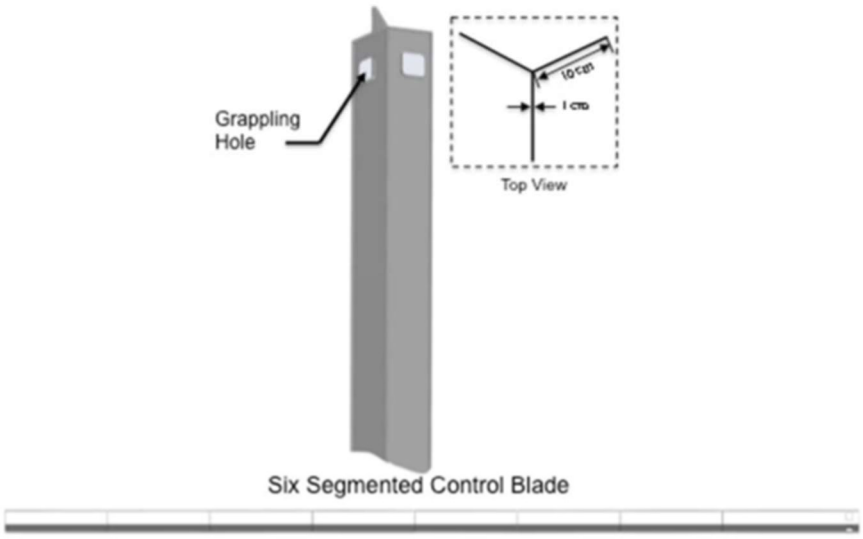

Figure 2-19: AHTR control blade geometry. (Varma, et al., 2012)

2.5.2. Grappling Collar and Drive Mechanism

The grappling collar (Figure 2-20) interfaces with upper plate and provides grappling interface for fuel handling.

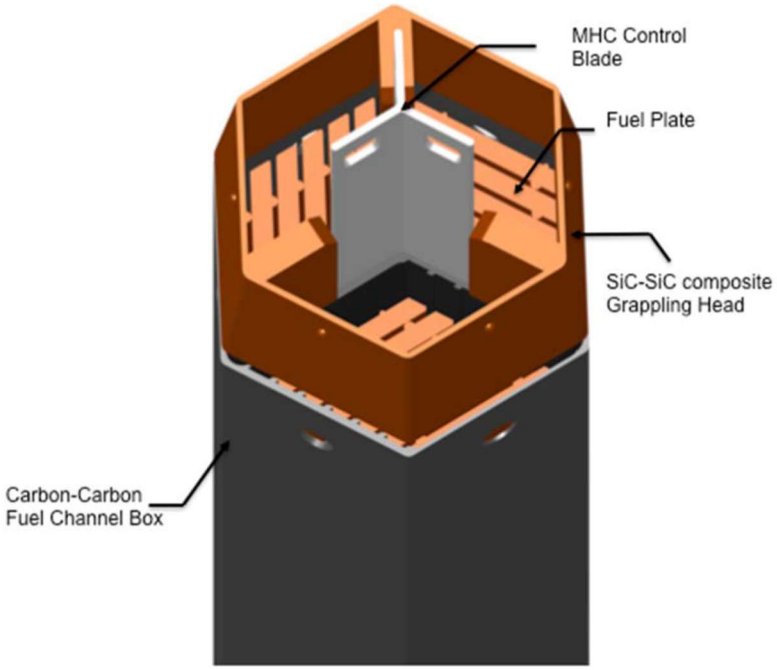

Figure 2-20 AHTR grappling collar in detail. (Varma, et al., 2012)

Each control blade has a leader rod that extends from the top of the control rod to the vessel flange. Each leader rod is encased in a control blade guide tube (Figure 2-21). Leader rod and guide tube are made of SiC-SiC composite.

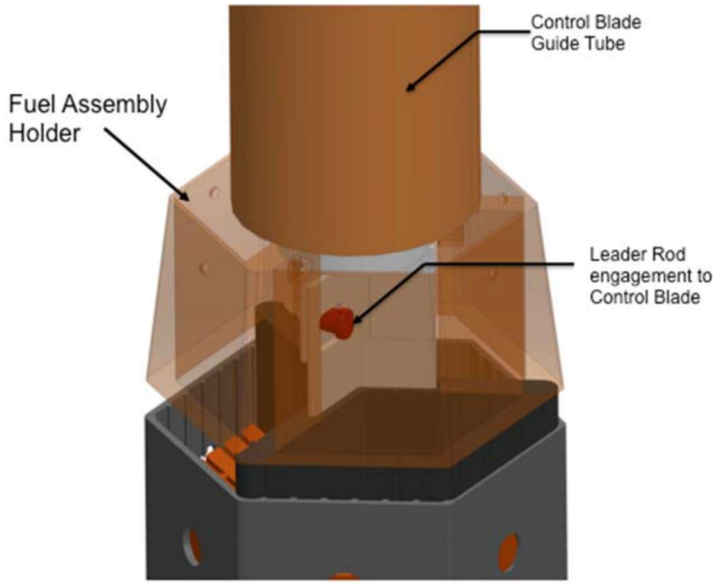

Figure 2-21 Guide tube and grappling collar in detail. (Varma, et al., 2012)

2.6. Fuel Plate

The LSCR fuel plank is shaped as a parallelepiped with two fuel stripes sandwiching a central carbon slab. There is a thin 1mm pyrocarbon sleeve around the fuel stripes to prevent erosion of TRISO particles. The TRISO fuel particles are randomly dispersed within the fuel strip with a 40% packing fraction in the 2011 model. (Holcomb, et al., 2011) This can be modeled with a TRISO spherical square lattice with a pitch of 0.09265 cm. The newer 2012 reference design has a carbon to heavy metal ratio that is twice as high at 400 compared to the 2011 design. (Varma, et al., 2012) It also has 9 wt% enrichment down from 19.75 wt% enrichment in the preliminary preconceptual design. The enrichment was lowered to reduce the fuel cycle cost and initial capital investment. The 9 wt% enriched fuel has a Carbon to Heavy Metal (CHM) ratio of 400 in the 2012 preconceptual design. The fuel stripe could be made smaller or the packing fraction can be reduced to produce a higher CHM ratio. It is recommended that the fuel stripe thickness be set to contain six fuel layers and a 20% packing fraction. This gives a square pitch of 0.116736 cm. High density graphite matrix is inside the fuel stripe in between the TRISO particles. The density of the carbon matrix is 1.75 g/cm^3. Burnable poison particles included near the center of the plate. There are two semi-cylindrical spacers on each of the fuel planks. Figure 2-23 gives a general idea of the configuration of the plate; Figure 2-23 and Figure 2-24 present the dimensions of the plate.

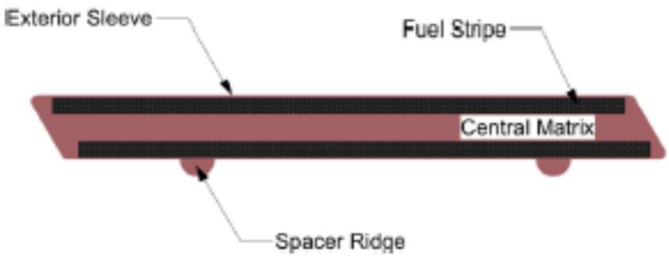

Figure 2-22: Geometrical configuration of the AHTR fuel plate. (Varma, et al., 2012)

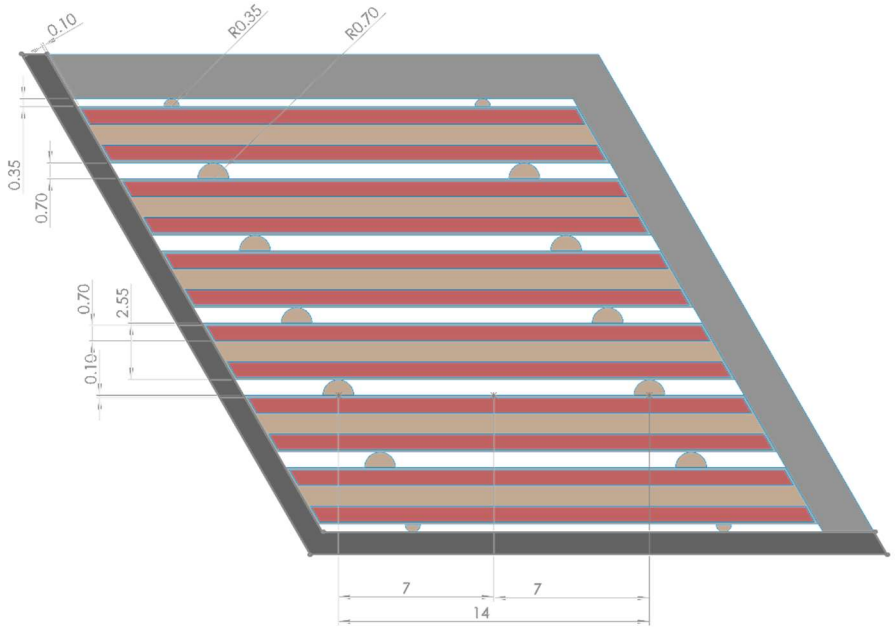

Figure 2-23: Dimensions of the AHTR fuel plate. (Varma, et al., 2012)

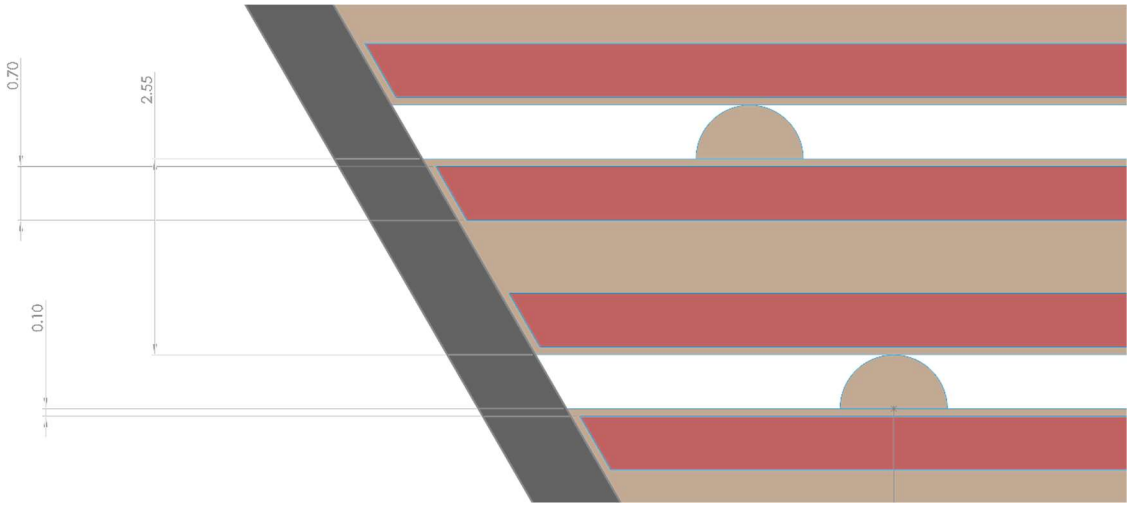

Figure 2-24: Dimensions of the AHTR fuel plate in detail. (Varma, et al., 2012)

2.6.1. TRISO Particle

The TRISO fuel particle consists of four layers, an outer pyrocarbon layer, silicon carbide layer, an inner pyrocarbon layer, and a less dense carbon buffer layer. Inside of these layers is a uranium oxycarbide fuel kernel, Figure 2-25 shows the geometry with the outer layers cut out of the TRISO fuel particle. This fuel is the same as the Advanced Gas Reactor (AGR) fuel developed under DOE-NE sponsorship. The reference irradiation experiment for the fuel type used for the AHTR is AGR-5/6. Fuel enrichment is 9 wt%. Table 2-4 shows the respective dimensions of the TRISO fuel particle.

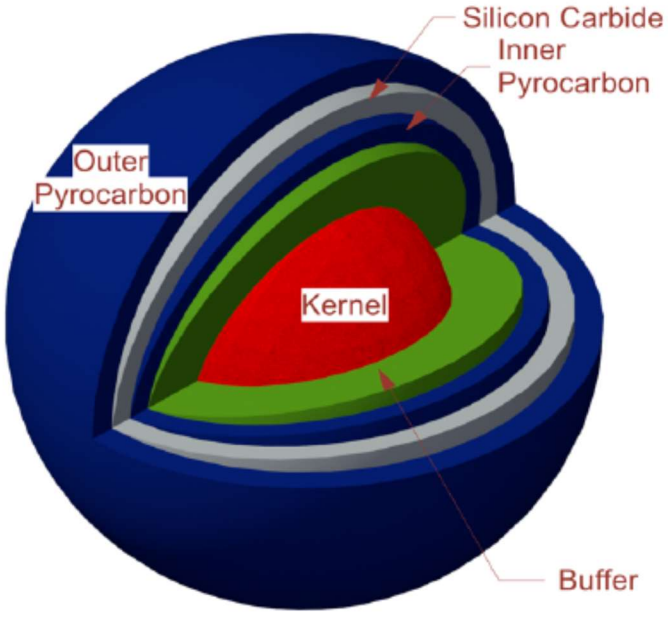

Figure 2-25: TRISO particle geometry configuration. (Varma, et al., 2012)

Table 2-4: TRISO particle parameters.

Region	Parameter	value μm	Material	ρ (g/cm^3)
Kernel	diameter	427	UCO	10.9
Buffer	thickness	100	Porous graphite	1
IPyC	thickness	35	Pyrolitic graphite	1.9
SiC	thickness	35	SiC	3.2
OPyC	thickness	40	Pyrolitic graphite	1.87
Fuel Particle	diameter	847	----	----

2.6.2. Burnable Poison

The burnable poison is located in Pyrocarbon overcoated sintered grains of Eu_2O_3 powder; these grains are placed at the center of the plate (Figure 2-26).

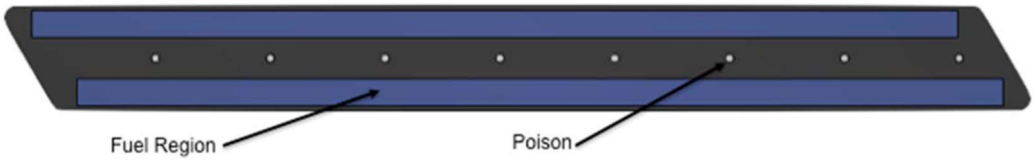

Figure 2-26: Burnable poison grains in the AHTR fuel plate. (Varma, et al., 2012)

Eu_2O_3 has high thermal stability. The melting point is 2,350°C and the density of Eu_2O_3 is 5.0 g/cm^3 (68% of theoretical density). The size and number of Eu_2O_3 grains can be optimized (although, studies available are not very accurate). The final reference design would be 5 grains with radius of 350 micron, In order to provide the required 6 months cycle. (Varma, et al., 2012) For this configuration, the excess reactivity of the core is maintained below 5% for the entire equilibrium cycle.

2.7. Primary Coolant

FLiBe ($2LiF\text{-}BeF_2$) is used as coolant for the primary system and flows over the AHTR core. The Beryllium provides some moderation, while the lithium is ideally isotopically pure ^7Li to minimize tritium production. 99.995 wt% ^7Li enrichment is generally considered the reference enrichment that can be practically achieved. The salt is transparent and has a density of 1,950 kg/m^3 at 700°C (it is temperature dependent) and a melting point of 459°C. Thus the salt is in the liquid phase in the primary loop while the reactor is operating, since the core inlet temperature is considered to be 650°C.

3. A Literature Review of Previous AHTR Neutronics Modeling and Simulation Methods/Tools

This section provides a literature review of on neutronics modeling and simulation tools, methods, and codes that have been applied to the AHTR reactor preconceptual design. Additionally, relevant analysis of other FHR systems has been incorporated, as there are similar challenges with double heterogeneity, FLiBe interaction, and graphite interaction between various reactor designs. This section highlights some of these challenges and presents a current status report of research in these areas.

3.1. Phenomena of Interest for Modeling FHRs

Several challenges for accurately modeling the AHTR and other FHR technologies have been identified and discussed in the literature. This section addresses some of the major areas of concern for neutronics modeling.

3.1.1. Double Heterogeneity

The issue of double heterogeneity arises from the introduction of the TRISO fuel particles into the reactor design. These TRISO particles form the first level of heterogeneity, as they consist of four layers; an outer pyrocarbon layer, silicon carbide layer, an inner pyrocarbon layer, and a less dense carbon buffer layer. Inside of these layers is a uranium oxycarbide fuel kernel (Figure 2-25). The second level of heterogeneity arises from the fuel elements themselves. The TRISO particles are packed into fuel stripes, which are contained within fuel plates that are heterogeneous with the coolant, moderator, and reflector regions. (Goluoglu & Williams, 2005)

The computational time required to explicitly model individual TRISO particles in the reactor makes this approach time consuming, costly, and impractical for the majority of applications. Applying a simple volume or flux weighted homogenization has proven to be insufficient for TRISO particle, due to the resonant self-shielding effect of the kernel and coated layers. The TRISO particle was originally developed for use in the HTGR and several methods for homogenization of the TRISO particle have been explored for use.

3.1.1.1. Reactivity-Equivalent Physical Transformation (RPT) Method

The Reactivity-Equivalent Physical Transformation (RPT) method is an effective way to model a system that uses coated TRISO particles. (Kim & Baek, 2005) The RPT method models the fuel by collecting the TRISO particles in a smaller active RPT region and then performing a volume-weighted homogenization on the transformed active region. (Cisneros & Ilas, 2012) This method was originally implemented to study HTGRs with spherical and cylindrical fuels, however it has been applied to the AHTR to look at depletion analysis. (Kim & Baek, 2005) (Cisneros & Ilas, 2012) (Kim & Venneri, 2008)

The design of the AHTR fuel plate (Figure 2-22) can be represented by a layered slab, since the plate contains two well defined stripes of TRISO particles surrounding a carbon slab. The layered slab transformation proved to more accurately represent the solution compared with the reference model for the AHTR. (Cisneros & Ilas, 2012) Figure 3-1 depicts the RPT homogenization process.

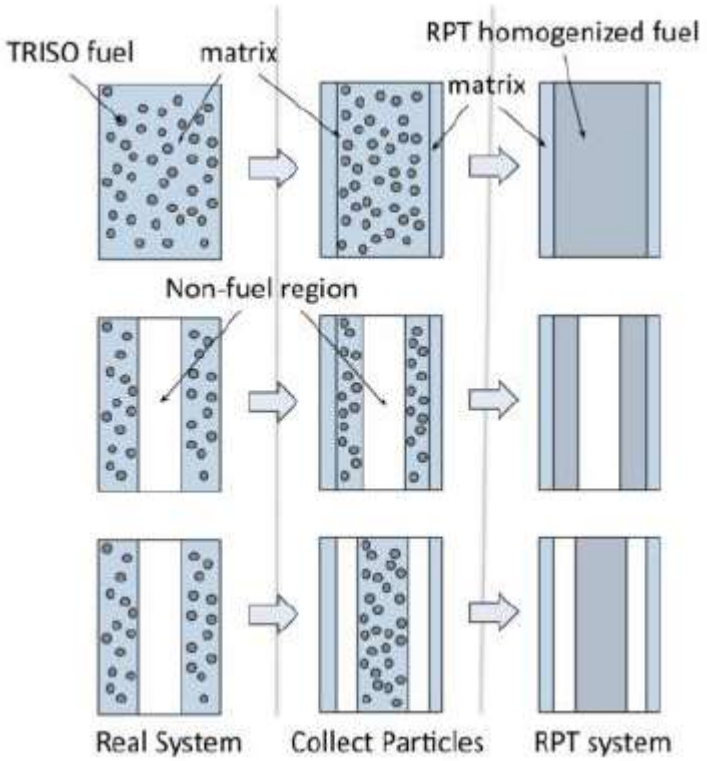

Figure 3-1: RPT method volume homogenization representation for slab geometries. (Cisneros & Ilas, 2012) Top – Solid Slab; Middle – Layered Slab; Bottom – Solid Slab Approximation

3.1.1.2. Dancoff Correction Method

The Dancoff Correction Method provides a correction to the escape probability of a neutron born in a fuel lump to account for the shielding effect from other nearby absorbers. (Bell & Glasstone, 1970) This method is similar to RPT, however instead of selecting equivalent dimensions, and equivalent Dancoff factor is selected to force the initial critical state to match the reference. (Kelly & Ilas, 2012) This method was applied to the CENTRM module of the SCALE code system, which is used for cross section processing and applied to the AHTR core.

One major advantage of the Dancoff Correction Method is that a distribution of Dancoff factors can be calculated and applied to different regions of the reactor, improving the spatial prediction of various quantities. (Kelly & Ilas, 2012) Additionally, this method has proven to work for configurations where the RPT method is incapable of determining an equivalent dimension, such as the case of high carbon-to-heavy-metal ratios that exist in AHTR configurations. (Kelly & Ilas, 2012)

3.1.2. FLiBe Spectrum and Cross-Sections

FLiBe ($2LiF\text{-}BeF_2$) is used as coolant for the AHTR and displays several advantages as a coolant. However, for neutronics analysis the use of FLiBe presents several challenges related to reactor physics phenomena arising from the use of FLiBe as a coolant in the AHTR, including:

- FLiBe contribution to neutron moderation
- Reactivity feedback (temperature/void)
- Concentration of ^6Li in the FLiBe – effects tritium production and is a strong thermal neutron poison
- Uncertainties in nuclear data for FLiBe constituents

The four constituents of FLiBe are ^6Li, ^7Li, Be, and F. There is significant uncertainty in the capture cross section for ^7Li, since its capture daughters are difficult to detect and capture in elemental lithium is dominated by ^6Li, directly impacting the FLiBe's contribution to moderation. While the initial FLiBe will strive to contain 99.995 wt% enriched ^7Li and the minute amounts of ^6Li present initially should burn out quickly, it continues to be produced via a ^9Be (n, α) ^6Li reaction. The rate of ^6Li production and destruction depend on the neutron spectrum of the AHTR core, and the accuracy of its concentration is essential to determining the reactivity feedback effects from the coolant. The destruction of ^6Li is more probable with a soft reactor spectrum, while its production is more probable with a hard neutron spectrum. Additionally, it is unknown if there is an effect on the FLiBe cross sections from the use of current F cross sections, since the fluorine in the FLiBe is bound as a salt and not a free gas. Lastly, since many of the neutronics codes used will rely on Monte Carlo methods, lack of S (α, β) data may have an effect on the accuracy of the criticality models.

3.1.3. Complex Geometry of AHTR

Many neutronics codes were designed with traditional Light Water Reactors (LWR) in mind, and any deviation from the traditional fuel pin in a square lattice can be difficult to represent. The AHTR design requires high fidelity modeling of fuel plates, hexagonal fuel assemblies, y-shaped control rods, TRISO fuel, and other core components all coupled together with a variety of shapes. Any neutronics code used to model the reactor system must be able to accurately represent the complex nature of the reactor.

3.2. Candidate Neutronics Codes for AHTR Analysis

Give the complex nature of the AHTR geometry and issues related to accurately capturing the physics of phenomena such as double heterogeneity and random TRISO particle packing, several code packages have been identified as having the potential to analyze the AHTR core neutronics. All code packages are either available from the Radiation Safety Information Computational Center (RSICC) located at ORNL, or are in house codes developed by IRP members.

3.2.1. SCALE

The Standardized Computer Analyses and Licensing Evaluation (SCALE) code is developed and maintained by ORNL. The SCALE code system consists of sets of modules and can be applied to solve criticality, shielding, radiation source term, spent fuel depletion/decay, reactor physics, and sensitivity/uncertainty analyses problems and is available through RSICC. (SCALE, 2011) The SCALE code has been applied to the AHTR to evaluate homogenization of TRISO particles, core physics calculations, burnup, and evaluate reactor feedback coefficients. (Cisneros & Ilas, 2012) (Holcomb, et al., 2011)

3.2.2. MCNP

The general-purpose Monte-Carlo N-Particle (MCNP) code can be used for neutron, photon, electron, and coupled particle transport and was developed at Los Alamos National Laboratory and available through RSICC. (MCNP, 2013) MCNP utilizes pointwise cross-section data, however multi-group calculations can be performed. MCNP's wide range of geometry definitions make it an excellent choice to represent the complex nature of the AHTR reactor. MCNP has a proven history with modeling systems containing TRISO particles and has been applied other FHR systems for core physics calculations.

3.2.3. SERPENT

SERPENT is a continuous energy Monte Carlo reactor physics burnup calculation code, developed by VTT Technical Research Centre of Finland and distributed by RSICC in the United States. (Leppänen, 2015) SERPENT functions similarly to other major Monte Carlo codes, such as MCNP and the KENO module of the SCALE code system, but it provides additional features for fuel design purposes. SERPENT has been used to model systems with TRISO fuel particles explicitly. (Suikkanen, Rintala, & Kyrki-Rajamäki, 2010)

3.2.4. COMET

COMET is a Georgia Tech advanced hybrid stochastic and deterministic transport code with stochastic method fidelity such as those in MCNP and SERPENT but with computational speeds several orders of magnitude faster. COMET works by decomposing a large, heterogeneous system into a set of smaller fixed source problems. For each unique local problem that exists, a solution called the response function is obtained. These response functions are pre-computed as a library for future use when resolving the set of smaller fixed source problems. The overall solution to the global problem is then obtained by a linear superposition of these smaller local problems. COMET's computational efficiency and ability to model complex geometries make it an ideal candidate for AHTR neutronics modeling. COMET has been proven highly accurate for traditional Light Water Reactors (LWR), Pebble Bed Reactors (PBR), the Very High Temperature Reactor (VHTR) and the HTGR at steady state.

4. Parameters of Interest in Neutronics Modeling and Simulation of the AHTR

In the process of developing the preconceptual design for the AHTR at ORNL, several areas of interest were explored and included in the design reports and/or published as separate papers. These include a preliminary core depletion calculations, reactivity feedback effects from temperature and void. A brief synopsis of this research is presented in this chapter.

4.1. Depletion Analysis

The 2012 revision of the AHTR preconceptual design refined the baseline AHTR fuel design. In particular, the fuel enrichment was lowered to 9 wt% and the CHM atomic ratio was increased to 400. (Varma, et al., 2012) Additionally, a higher density carbonaceous matrix material (1.75 g/cm^3) was employed in the fuel. These changes resulted in the adoption of a two-batch fuel cycle with a 1 year in-core fuel residence time. The results from the 2011 preconceptual design were depicted in several publications, discussing the calculation methods using SCALE. (Holcomb, et al., 2011) (Cisneros & Ilas, 2012) The resulting two-batch fuel cycle adopted a checkerboard refueling pattern (Figure 4-1), where every other fuel assembly in a given assembly ring is replaced by a fresh fuel assembly and there is not fuel in the central assembly.

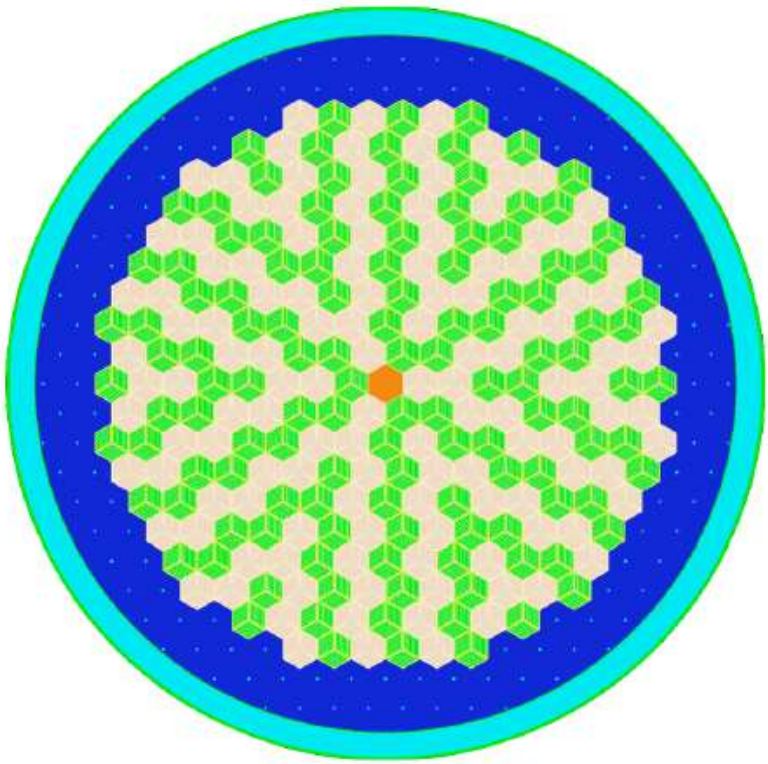

Figure 4-1: AHTR two-batch checkerboard refueling pattern. (Varma, et al., 2012)

The two-batch fuel cycle design from the 2012 AHTR preconceptual design results in the main core characteristics provided in Table 4-1. The fuel management scheme for the two-batch fuel cycle was initially calculated with a Linear Reactivity Model (LRM) and then simulated via a direct calculation. (Varma, et al., 2012) Figure 4-2 depicts the reactivity as a function of fuel residence time, with the direct calculation providing a slightly higher reactivity reserve at the end of the 6-month, two-batch cycle.

Table 4-1: AHTR core power and burnup characteristics.

Parameter	Value	Units
Power (thermal)	3400	MW
Power per TRISO (average)	77	mW/particle
Power Density (average)	97	W/cm^3
Volumetric Core Power Density	12.9	MW/m^3
Heavy Metal Mass (fresh core)	17.48	MT
Fuel Residence Time (two-batch)	1.0	yr
Discharge Burnup (average)	71	GWd/MTHM

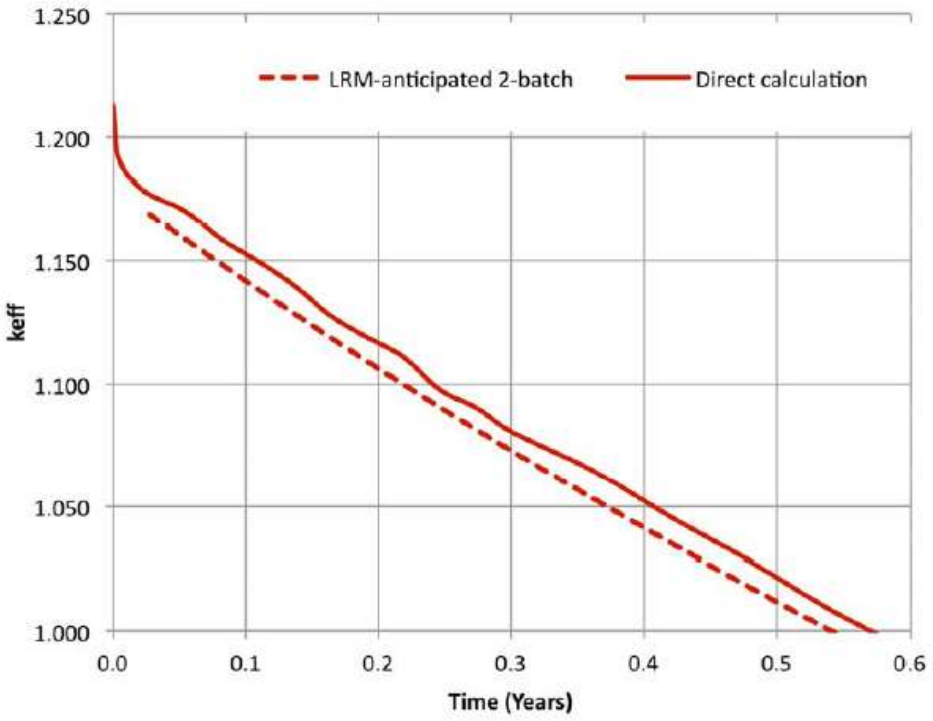

Figure 4-2: AHTR two-batch fuel cycle multiplication constant as a function of burnup. (Varma, et al., 2012)

4.2. Reactivity Feedback Coefficients

4.2.1. Isothermal Reactivity Coefficient

The isothermal (uniform temperature everywhere) reactivity coefficient was evaluated for both the 2011 and 2012 preconceptual designs at the beginning of the initial cycle and over a wide temperature interval, using the methodology applied in (Ilas, 2012). (Varma, et al., 2012) Figure 4-3 shows the behavior of the isothermal reactivity coefficient, which increases with increasing temperatures but remains negative with a good amount of margin for all potential operating temperatures.

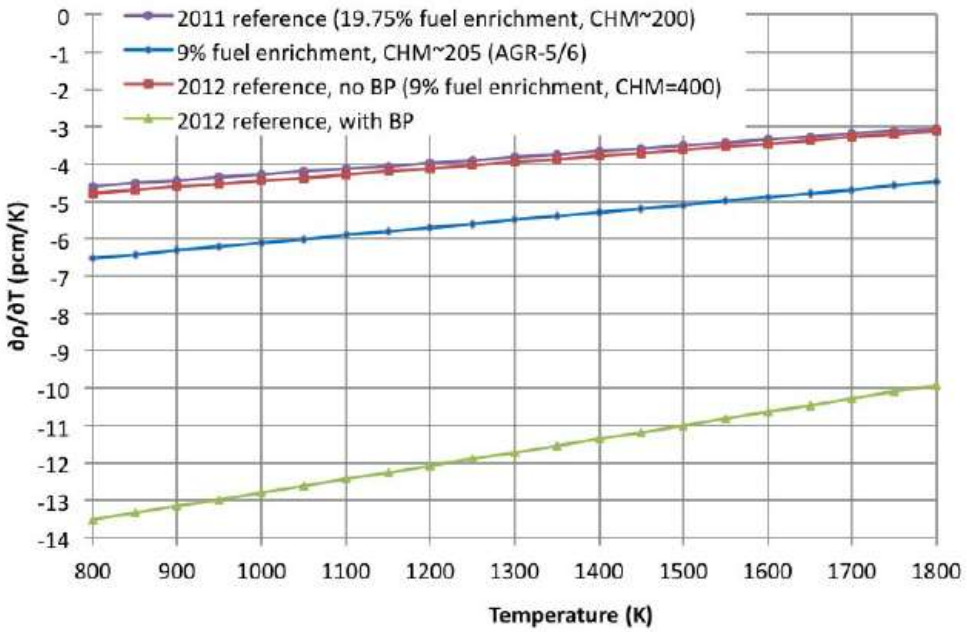

Figure 4-3: AHTR isothermal temperature reactivity coefficient. (Varma, et al., 2012)

The introduction of the burnable poison to the 2012 AHTR design resulted in a significant decrease in the isothermal reactivity coefficient. Thus, it was important to analyze the isothermal reactivity coefficient at additional points in the two-batch fuel cycle. Since the burnable poison is consumed, the excess negativity would be reduced as one progresses through the fuel cycle. Figure 4-4 provides the behavior of the isothermal temperature coefficient of reactivity at the end of the initial core cycle (EOC1) and at the beginning of the second equilibrium cycle (BOC2). Observing the trend presented in Figure 4-4, at operating temperatures the isothermal temperature reactivity feedback coefficient remains negative throughout the two-batch fuel cycle.

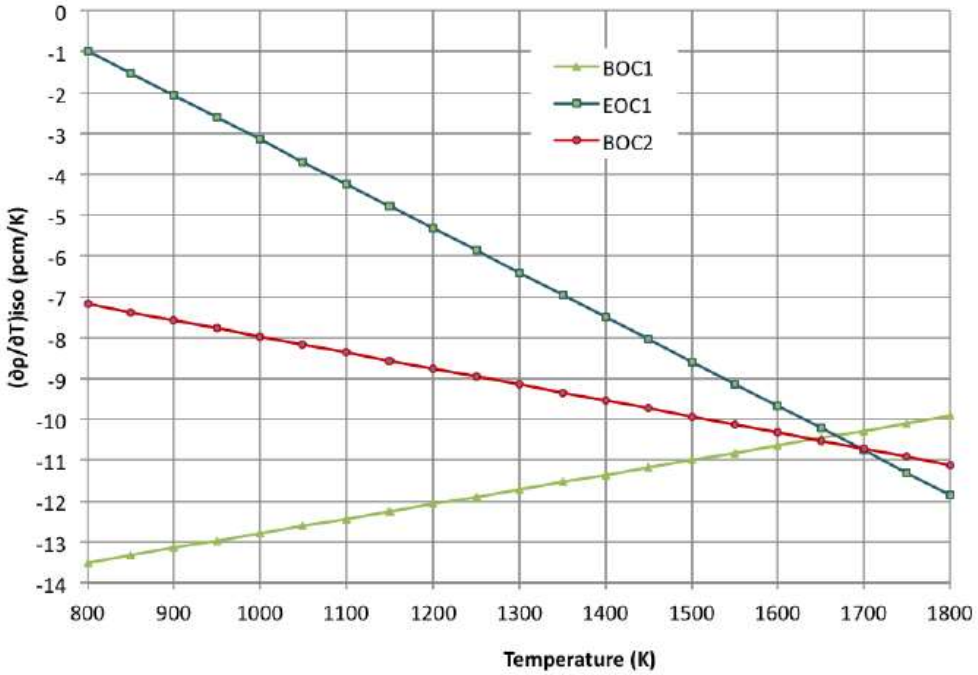

Figure 4-4: AHTR isothermal temperature reactivity coefficient at different points in the fuel cycle. (Varma, et al., 2012)

4.2.2. Void Reactivity Coefficient

As with the isothermal reactivity coefficient, the void reactivity coefficient was re-evaluated for the 2012 AHTR preconceptual design. The resulting void reactivity coefficients (Figure 4-5) were calculated at the beginning of cycle for the initial core (with and without burnable poison), at the end of cycle for the initial core, and at the beginning of the equilibrium core as a function of void fraction. The addition of burnable poison to the fuel plates results in a non-linear behavior of the void reactivity coefficient. Additionally, this results in changes of sign for different void fractions. (Varma, et al., 2012)

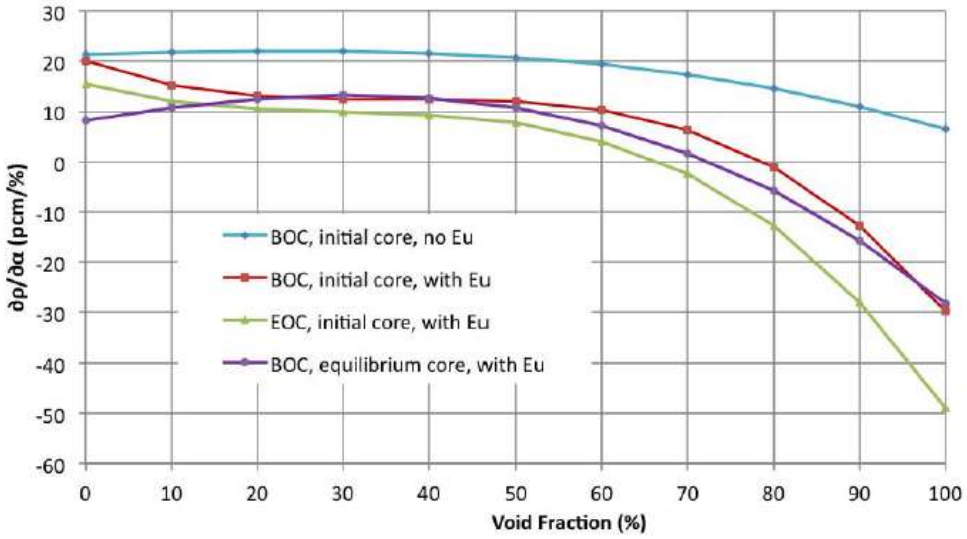

Figure 4-5: AHTR coolant void reactivity coefficient. (Varma, et al., 2012)

Since and increase in fuel temperature will result in a decrease in coolant density, the fuel temperature reactivity coefficient must be more negative than the coolant thermal density decrease is positive. (Varma, et al., 2012) To ensure the overall core temperature coefficient remains negative under all conditions, the isothermal reactivity coefficient must be more negative than -1 pcm/K. From the core conditions analyzed in Figure 4-4, this condition is always true.

5. Phenomena Initially Identified for Discussion at PIRT-like Exercise

DISCLAIMER: This section attempts to highlight some of the phenomena initially identified as discussion points for the PIRT-like exercise. This list is in no way a complete description of potential phenomena and may include items which have little or no relevant effects on calculations. These items serve only as a preliminary basis for discussion and will be expanded on by the panel.

- Modeling of the TRISO particles
- Modeling of carbon containing components and structures
- How to account for double heterogeneity
- Accuracy of Fluorine scatter cross sections
- Effect of the use of Florine cross sections based on gaseous Fluorine when to represent the bound Fluorine in FLiBe
- AHTR neutron spectrum
- Effect of ^{6}Li concentration on neutron moderation and reactivity feedback
- Concentration of ^{6}Li in FLiBe as the reactor operates
- S (α, β) for FLiBe
- Effects of the 50°C ΔT in coolant over the core for neutronics modeling

References

Bell, G., & Glasstone, S. (1970). *Nuclear Reactor Theory.* New York, NY: Van Nostrand Reinhold Company.

Cisneros, A. T., & Ilas, D. (2012). Neutronics and Depletion Methods for Parametric Studies of Flouride-Salt-Cooled High-Temperature Reactors with Slab Fuel Geometry and Multi-Batch Fuel Management Schemes. Knoxville, TN: PHYSOR 2012 - Advances in Reactor Physics - Linking Research, Industry, and Education.

Goluoglu, S., & Williams, M. L. (2005). Modeling Doubly Heterogeneous Systems in SCALE. Washington, D.C.: Transactions of the American Nuclear Society.

Holcomb, D. E., Ilas, D., Varma, V. K., Cisneros, A. T., Kelly, R. P., & Gehin, J. C. (2011). *Core and Refueling Design Studies for the Advanced High Temperature Reactor (ORNL/TM-2011/365).* Oak Ridge, TN: Oak Ridge National Laboratory.

Ilas, D. (2012). SCALE Code Validation for Prismatic High-Temperature Gas-Cooled Reactors. Knoxville, TN: PHYSOR 2012 - Advances in Reactor Physics - Linking Research, Industry, and Education.

Kelly, R., & Ilas, D. (2012). Verification of a Depletion Method in SCALE for the Advanced High Temerature Reactor. Knoxville, TN: PHYSOR 2012 - Advances in Reactor Physics - Linking Research, Industry, and Education.

Kim, Y., & Baek, M. (2005). Elimination of Double-Heterogeneity through a Reactivity-Equivalent Physical Transformation. Tsukuba, Japan: Proceedings of Global 2005.

Kim, Y., & Venneri, F. (2008). Optimization of One-Pass Transuranium Deep Burn in a Modular Helium Reactor. *160*(1), 59-74.

Leppänen, J. (2015). *SERPENT - A Continuous Energy Monte Carlo Reactor Physics Burnup Calculation Code.* VTT Technical Research Centre of Finland.

MCNP. (2013). Monte Carlo N-Particle Transport Code. *Version 6.1*. Los Alamos, NM: Los Alamos National Laboratory.

SCALE. (2011). A Comprehensive Modeling and Simulation Suite for Nuclear Safety Analysis and Design (ORNL/TM-2005/39). *Version 6.1*. Oak Ridge, TN: Oak Ridge National Laboratory.

Suikkanen, H., Rintala, V., & Kyrki-Rajamäki, R. (2010). An Approach for Detailed Reactor Physics Modeling of Randomly Packed Pebble Beds. *Proceedings of HTR 2010.* Prague, Czech Republic.

Varma, V. K., Holcomb, D. E., Peretz, F. J., Bradley, E. C., Ilas, D. Q., & Zaharia, N. M. (2012). *AHTR Mechanical, Structural, and Neutronic Preconceptual Design (ORNL/TM-2012/320).* Oak Ridge, TN: Oak Ridge National Laboratory.